SECED 2023 Conference
Earthquake Engineering & Dynamics for a Sustainable Future
14-15 September 2023, Cambridge, UK

SEISMIC FRAGILITY ANALYSIS OF PWR SPENT FUEL POOL

Stoyan ANDREEV[1], Manya DEYANOVA[2], Tsvetan GENOV[3], Joao Paulo TRAVANCA[4]& Anton ANDONOV[5]

Abstract: *This paper presents the methodology, analysis, and the main results from a study for assessing the seismic fragility of a Spent Fuel Pool (SFP) found in typical existing PWR units. The study covered the reinforced concrete structure and the stainless steel liner of the SFP in order to find the minimum HCLPF value representative for the whole facility. A graded approach for calculating the HCLPF with increasing sophistication and decreasing conservatism was implemented, based on EPRI TR-3002012994 and EPRI TR-3002009564 supplemented by nuclear industry analysis and design standards. Due to the robustness of the pool reinforced concrete walls and floor, their capacity was estimated using the Conservative deterministic failure margin (CDFM) method. The SFP reinforced concrete structure was demonstrated to be robust with a HCLPF value of 2.05g. The critical structural failure mode is shear of the SFP floor, which may lead to gross structural failure and uncontrollable loss of SFP inventory water. To assess the liner fragility a total of 11 failure modes were considered, covering all components of the liner systems and their connections and anchoring. For each mode, the median capacity, the randomness, and uncertainty were calculated in order to estimate the HCLPF. The stress distributions and the deformations of the liner components were estimated from a series of 3-D non-linear dynamic analyses of a coupled model of the SFP including the RC structure, the steel liner, the spent fuel racks, and the inventory water. The minimum HCLPF for liner failure was found to be 0.88g. The effect of potential correlation between liner failure modes was found to be negligible.*

Introduction and high-level methodology

Study objective, scope and input data

The main objective of the presented study is develop a probabilistic definition of the capacity of a typical Spent Fuel Pool (SFP) found in many Western type Pressurized Water Reactors (PWRs) to withstand earthquakes. Such definition, including median capacity (A_m), randomness (β_R) and uncertainty (β_U), or the High Confidence for Low Probability of Failure (HCLPF) capacity are used as input to evaluate the contribution of external events to the probability of fuel damage for the power plant and in designing further safety improvements.

The study includes analysis and evaluation of the seismic fragility of both the SFP reinforced concrete structure (walls and slabs) and its leak-tight liner, as failure of any of those components will lead to uncontrolled loss of inventory water, contamination of adjacent rooms in the reactor building and potential heat built up in the stored spent fuel.

The input for the study is based on available data for generic SFP located in many PWRs. Where required data was not available, the gaps were bridged based on the provisions in the applicable nuclear codes and standards. For the needs of the study, a reference earthquake (RE) level consistent with an area of moderate to high seismicity (PGA=0.6g) was used as threshold for comparison of estimated fragilities.

Spent Fuel Pool geometry and inventory

[1] Principal structural engineer, Mott MacDonald, Sofia, Bulgaria, stoyan.andreev@mottmac.com
[2] Principal seismic engineer, Mott MacDonald, Sofia, Bulgaria
[3] Structural analyst, Mott MacDonald, Sofia, Bulgaria
[4] Principal structural analyst, Mott MacDonald, Sofia, Bulgaria
[5] Technical director, Sofia, Bulgaria

The SFP consists of a reinforced concrete box structure with dimensions L=16.54m, B=7.93m, and H=12.67m and steel liner on the inside of the floor and walls. The floor slab of the pool is 2.00m thick, and all the walls are 1.83m thick. The normal operational water level in the pool was assumed to be 0.46m below the edge. The SFP is an integral part of the reactor building. The

SFP floor slab is supported by the surrounding walls in longitudinal direction, and transverse direction, and by one intermediate wall. Two of the SFP walls are supported in their transverse direction (see Figure 1). The SFP is located at a lower elevation in the reactor building, with only one storey between it and the basemat of the building.

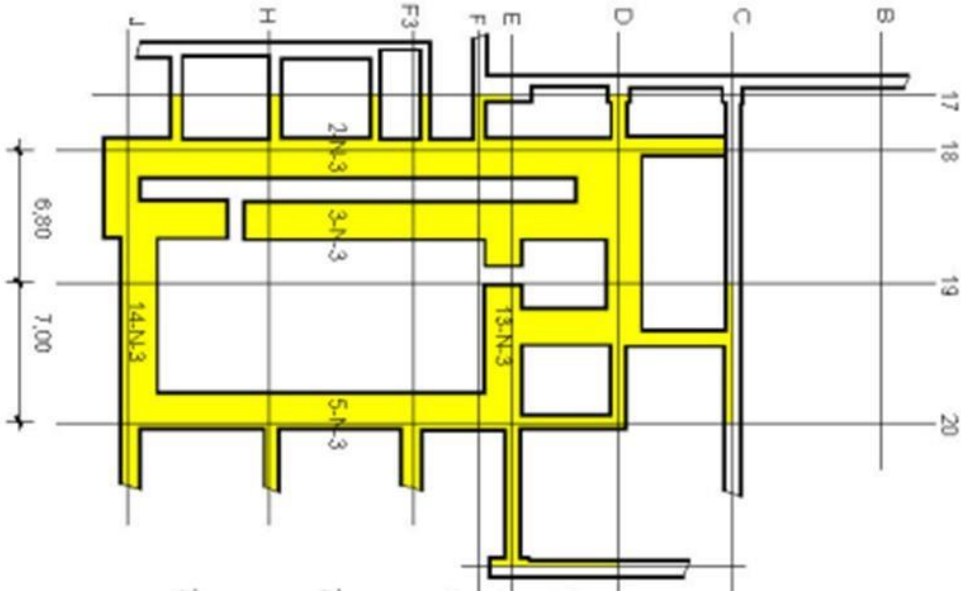

Figure 1. Plan layout of the SFP considered in this study

The inventory of the SFP includes the water (~1600m^3) and a large number of fuel racks containing the fuel assemblies stored in the pool. The racks are supported on the floor of the SFP and are not anchored to it, so they are allowed to move during a strong earthquake. The feet pf the racks are resting on baseplates welded to the floor liner. The leak-tightness of the SFP is assured using a stainless steel liner comprising of four main components:

- Liner plates, which are welded to embedded angles and anchor plates
- Embedded angles
- Anchor plates

In order for the liner to lose its leak-tightness function, the liner plates or the splices between them need to fail. Gross structural failure of the SFP floor or walls is expected to destroy the liner in a large area of the floor or wall and lead to rather quick uncontrolled loss of water and subsequent contamination of adjacent rooms in the reactor building and loss of cooling function for the spent fuel assemblies. Local failure of a line component (eg tearing of a liner plate) is expected to still lead to an uncontrolled loss of inventory water, but with rather slower leakage.

Overall approach to seismic fragility estimation

Graded approach to the assessment of the Spent Fuel Pool fragilities were applied as per EPRI TR-3002009564 and EPRI TR-3002012994:

- For the structural walls and slab, the Conservative Deterministic Failure Margin (CDFM) method was used for initial assessment of the structural HCLPF with simplified modelling of the seismic demand and conservative lower bound capacity of the SFP structure.
- The Separation of Variables (SoV) method was considered to be used for refinement of structural fragilities if the structural robustness could not be confirmed for the reference earthquake (RE) level. In this case, the seismic capacity was to be based on best estimate input and assumptions. The SoV method was not applied since the SFP structure was demonstrated to have sufficient margin of safety.
- For the liner component fragilities, the Separation of Variables method was directly implemented with seismic demand based on results from non-linear dynamic time history

analysis. The SoV method provided both HCLPF values and full families of fragility functions for the liner components failure

Seismic input for fragility assessment

The seismic input was defined in terms of probabilistic in-structure response spectra (PISRS) compatible with the selected intensity of the RE (anchored at PGA=0.6g) and the location of the SFP within a typical PWR reactor building. A sample PISRS used for the seismic fragility analysis is shown in Figure 2. When estimating the seismic demand and the acceleration (PGA) capacity, the PISRS were considered to be absolutely proportional to the PGA level, ignoring any nonlinear relations between them.

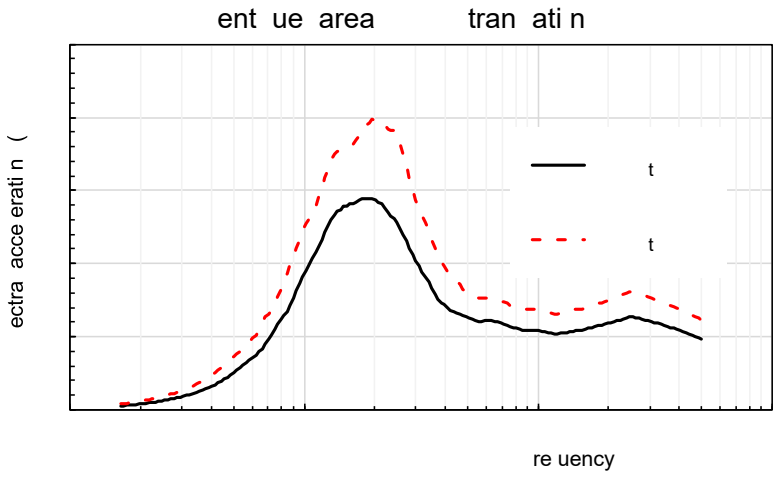

Figure 2. Sample PISRS for the SFP seismic fragility analysis

Simplified structural modelling of the SFP walls and floor slab

Two analytical SDOF models were considered for structural fragility evaluation: a) model of the SFP floor slab panel; and b) model of the wall, which has the largest span and no support from transverse walls and slabs (Figure 3). The dynamic degree-of-freedom of the models is out-ofplane vibration at the fundamental modes of the considered panels. The elastic stiffness of the panels was calculated based on elastic material properties and the respective boundary conditions (eg fixed edge). The elastic-plastic stiffness considers trilinear force-displacement backbone curves for flexure controlled panels and bilinear backbone curves for shear controlled panels.

The non-seismic load demand on the slab included its self-weight, the weight of the water as hydrostatic pressure and the weight of the spent fuel racks located in the SFP. For the walls, the water hydrostatic pressure and the self-weight was considered

The seismic load demand included inertial forces arising from vibrations of the panels (horizontal for walls, vertical for the floor slab), the inertial forces due to vibrations of the fuel racks and fuel assemblies (on the slab), and the earthquake-induced hydrodynamic water pressure on the walls and slab. The inertial forces were calculated as the product of the relevant vibrating mass (eg floor panel + fuel racks and fuel assemblies + water) and the peak acceleration for the frequency interval f_p±15%, where f_p is the best estimate panel out-of-plane frequency.

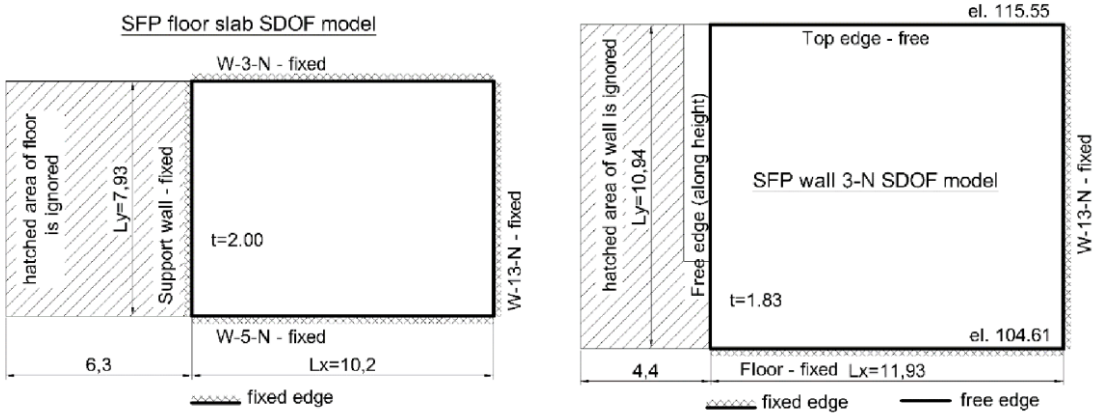

Figure 3. SDOF models for structural evaluation – floor slab (left); critical wall (right)

The hydrodynamic pressures on the floor and walls were calculated as per ACI 350.3. The loading effects on the floor slab from hydrodynamic pressures from horizontal and vertical seismic excitati n were c mbined u in t e " -40- " ru e in A C -16.

Detailed modelling and analysis of the SFP and its inventory

The detailed modelling and coupled dynamic analysis of the SFP was performed with LS-DYNA. The model development was compliant to the general and specific requirements of ASCE 4-16, Section 3. Only the SFP and some of the adjacent structural members were included in the 3D FEM. The strategy for which components to be included in the FE model and which to be excluded aimed at modelling the realistic boundary conditions and stiffening for SFP floor slab and walls and preserving their dynamic properties (see Figure 4).

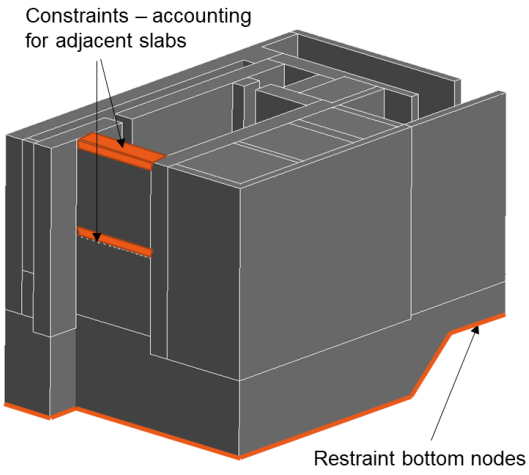

Figure 4. FEM of the SFP and adjacent walls and slabs

In order to capture the combined effects on the liner components due to imposed structural deformations and movement of fuel racks a coupled model capturing fluid-structure-equipment interaction was considered necessary. A complete model of the SFP facility including both special fluid elements and detailed FE representation of the racks and all possible fluid-structureequipment interactions was considered computationally inefficient. In lieu of this too sophisticated modelling, three separate FE models were used:

1. FE model with mass elements for fluid and fuel racks and assemblies. It has the fluid impulsive mass modelled with either vertical DOFs (for the floor) or horizontal DOFs (for the walls) mass elements distributed on the liner nodes. The convective fluid mass is modelled with a rigid volume connected to the liner nodes with distributed springs. The mass of the fuel racks and assemblies is distributed across the liner nodes on the floor.

   The model was used to assess the global and local dynamic response of the SFP and to demonstrate the applicability of the lumped mass model approach for the SFP fluid.
2. FE model with explicit modelling of the fluid inside the SFP and mass elements for fuel racks and assemblies. It has the fluid modelled using the Incompressible Fluid (ICFD)

formulation in LS-DYNA. The mass of the fuel racks and assemblies is distributed across the liner nodes on the floor. The model was used to assess the global and local dynamic response of the SFP and to demonstrate the applicability of the lumped mass model approach for the SFP fluid

3. FE model with mass elements for the fluid and finite element representation of the fuel racks. The fuel racks were modelled with finite element and had realistic geometry and support conditions (including contacts to the base plates and liner plates). This model was used to extract stresses and forces for the seismic fragility analysis of the liner components.

The different modelling approaches and model components are shown in Figure 5 to Figure 7. Further discussion of the detailed model of the SFP and the performed non-linear dynamic fluidstructure-equipment interaction analysis can be found in the accompanying paper at SECED23 by Genov et al. (2023).

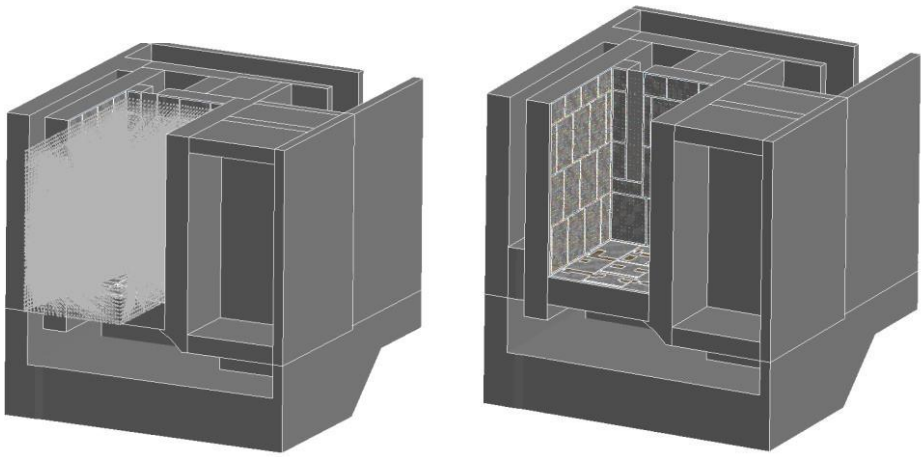

Figure 5. Modelling of convective fluid for FEM1 and FEM 3 (masses and springs)

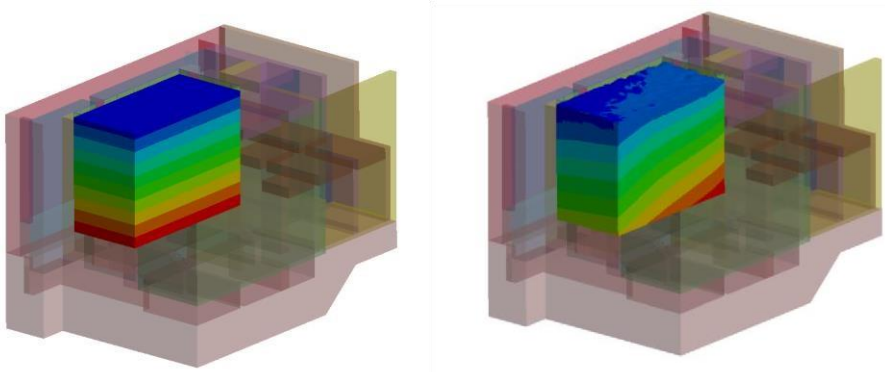

Figure 6. ICDF modelling of inventory fluid (FEM2)

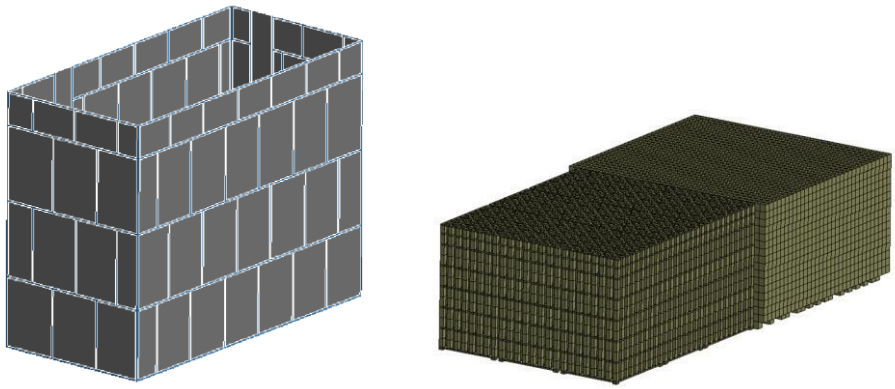

Figure 7. Modelling of liner (left) and fuel racks (right) in FEM3

CDFM assessment methodology for structural HCLPF estimation

The implementation of the CDFM method allows for quick and simple initial assessment that can be easily repeated for a large number of structural components in a Nuclear Power Plant for screening out of robust components and identification of components that are critical for safety. The CDFM method is suggested in EPRI TR-3002009564 since it was previously demonstrated that SFP structural components usually are robust and have sufficient margin even for high seismic demand.

In both the CDFM and SoV methods, the structural capacity factor F_C is calculated as the product of the elastic strength factor F_S and the ductility factor F_μ. The difference is that the for the CDFM analysis, lower bound values $F_{S,CDFM}$ and $F_{\mu\,CDM}$ are used, while for the SoV analysis the median values $F_{S,m}$ and $F_{\mu\,m}$ and the corresponding uncertainties should be calculated. The elastic strength factor FS for each structural component was calculated as per EPRI TR-3002012994:

$$F_S = \frac{R_U - D_{NS}}{E_{RE} - \Delta C_S} \quad (1)$$

In equation (1): R_U is the limiting panel elastic strength capacity, D_{NS} is the non-seismic demand, and E_{RE} is the seismic demand for the RE level. The parameter ΔC_S is the reduction or increase in capacity due to concurrent seismic loading. In the current calculations the c ntributi n ΔC_S was ignored because of the low axial stresses in the structural elements.

For the CDFM analysis the elastic strength factor $F_{S,CDFM}$ was based on the lower bound structural capacity $R_{U,CDFM}$ (~98% Non-exceedance probability) and seismic demand E_{RE84} with 84% NEP. According to EPRI TR-3002012994, the target 98% NEP of the capacity is achieved when using the code provided design strengths (eg from ACI 349). The material strengths f_{CDFM} in the code provided design equations were assumed to have 95% NEP, and the strength reduction factors ϕ_{CDFM} were assumed to have 84% NEP.

The spectral acceleration HCLPF capacity of each structural component is the product of the capacity factor F_C and the relevant peak in-structure spectral acceleration with 84% NEP at the fundamental mode of vibration of the component:

$$SA_{HCLPF,CDFM} = SA_{peak,RE84} \cdot F_{S,CDFM} \cdot F_{\mu,CDFM} \quad (2)$$

Since the peak spectral acceleration is proportional to the PGA, the RE free surface HCLPF PGA value was calculated directly as the product of the A_{RE}=0.6g and the capacity factor $F_{C,CDFM}$.

SoV assessment methodology for liner fragility estimation

The total safety factor for equipment F_E is the product of capacity factor Fc, structural response factor F_{RS} and equipment response factor F_{RE} as per EPRI TR-3002012994.

$$F_E = F_C \cdot F_{RS} \cdot F_{RE} \quad (3)$$

The structural response factor F_{RS} is modelled as the product of up to 13 factors influencing the structural response variability. The median values of the sub-factors and the corresponding randomness and/or uncertainty was based on EPRI TR-3002012994 (Table 5-7 of the document). The combined structural response factor for equipment fragility evaluation is F_{RS}=0.9, with β_R= 3 β_U= and β_C=0.38.

The equipment response factor considers both the response of the liner components and the spent fuel racks located in the SFP and includes five additional sub-factors based on EPRI TR3002012994, Section 5.5. The combined equipment response factor for fragility evaluation is F_{RE}= wit β_R= β_U= and β_C=0.21.

Structural fragilities using CDFM approach

Floor and wall panels flexural and shear strength

The nominal (unfactored) shear strength of the concrete sections was calculated per ACI 349M13 with consideration of 25% strength reduction due to thermal cracking.

The RC panels flexural capacity is calculated based on the yield line theory. The yield lines layout was varied until the minimum capacity was obtained. The representative yield lines layout for the is sketched in Figure 8.

The controlling failure mode of the floor slab panel is shear with the minimum capacity F_{US}=94.3MN (equivalent total force) or R_{US}=1.165MPa (equivalent pressure). The controlling failure mode is non-ductile with F_{μ}=1.0.

The controlling failure mode of the critical wall panel is flexure with the minimum force capacity F_{UF}=40.2MN (equivalent total force) or R_{UF}=0.308MPa (equivalent pressure). The controlling failure mode of the wall is ductile with the shear capacity ~50% higher than the flexure capacity.

Seismic and non-seismic demand on floor and wall panels

The vertical frequency of the floor slab was calculated to be f_{fl}=20.3Hz, or 17.25–23.34Hz considering the ±15% uncertainty. The RE peak vertical spectral acceleration at this interval is 0.93g and the total vertical pressure on the floor slab E_{FV}=0.252MPa, considering the combination of vertical and horizontal seismic excitation. The equivalent non-seismic pressure on the floor panels is D_{NS}=0.307MPa.

The out-of-plane frequency of the critical wall panel was calculated to be f_w=6.92Hz, or 5.89–7.96Hz considering the ±15% uncertainty. The RE peak vertical spectral acceleration at this interval is 0.67g. The convective mode of the water in transverse direction to the wall is 0.315Hz, with corresponding peak spectral acceleration of 0.46g. The combined horizontal pressure on the wall from convective and impulsive hydrodynamic pressure is E_{WC}=0.100MPa.

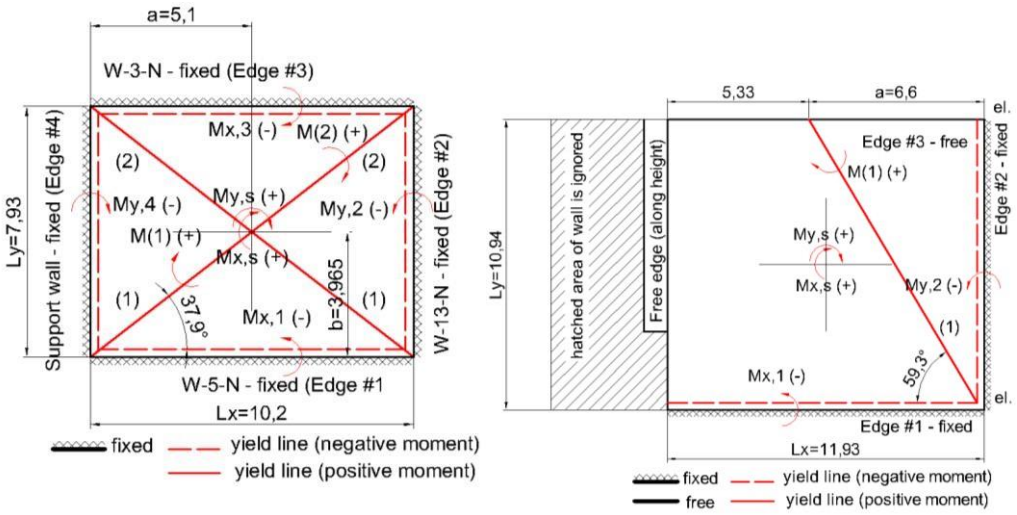

Figure 8. Yield lines for estimation of flexural capacity of floor panel (left) and wall panel (right) Structural HCLPF using the CDFM method

The elastic strength factor for the floor and wall panels are calculated from the minimum panel shear pressure capacity and the seismic and non-seismic load demand on the panels.

For the floor panel $F_{S,CDFM}$=1.88 and $F_{\mu,CDFM}$=2.0 for flexure, this the total margin factor is 3.76. The equivalent HCLPF for the wall is $A_{HCLPF,w}$=2.26g.

The minimum calculated CDFM HCLPF value is 2.05g for shear failure of the floor slab. This failure mode is representative for the whole SFP structure, as gross structural failure of the slab in shear will likely lead to both opening of wide cracks and tearing of significant section of the stainless steel liner, and thus rapid and uncontrollable loss of cooling water inventory.

Non-linear seismic analysis

Details of the non-linear seismic analysis are given in the accompanying paper at SECED23 by Genov et al. (2023).

Liner fragilities

The failure of the steel leak-tight liner was considered less severe than gross structural failure, since it is expected to be more localized thus the loss of inventory water to be slower. However,

such failure is not acceptable from safety perspective, so it needs to be ruled out on the basis of having sufficient margin of safety.

Failure modes

Initially, a total of 11 failure modes of four liner components were defined. After screening of their feasibility, a total of seven relevant failure modes were considered while the other were practically eliminated. The liner component capacities for each failure mode were based on the median code strength in the applicable codes ACI 349-13 and ANSI N690, with supplementary provisions of ANSI/ANS 57-7. Where applicable additional procedures (eg from EPRI TR-3002012994) were applied.

Liner component	**Failure mode**	**Relevant code or standard**
Liner plates	FM1. Liner plate tearing failure due to excessive inplane and transvers loading	AISC N690 ASME B&PV
	FM2. Liner bearing on concrete failure.	ACI 349
Racks base plates	FM5. Concrete bearing failure under base plates	ACI 349
Liner anchor plates	FM7. Concrete bearing failure of anchor plates	ACI 349
	FM8. Liner to anchor plate weld failure	AISC N690
Embedded angles at liner plate splices	FM9. Liner to embedded angle weld failure	AISC N690
	FM10. Concrete bearing failure of embedded angles	ACI 349

Table 1. Failure modes of liner components.

The tearing failure of the liner plates or their welds can be initiated by excessive in-plane stresses in the liner due to the combination of structural deformations and sliding friction from rack movement. The peak membrane stresses in the liner plates were directly obtained from the coupled non-linear dynamic analysis.

The concrete bearing failure modes (Figure 9) were of particular interests, since they could lead to local deformations of the liner (wrinkles or sagging) and subsequent tearing due to sliding of the racks feet. However, such complex failure modes are very hard to predict in practice, thus it was assumed that if concrete crushing is initiated, liner failure also occurs. The peak punching forces beneath the racks feet were obtained from the coupled non-linear dynamic analysis.

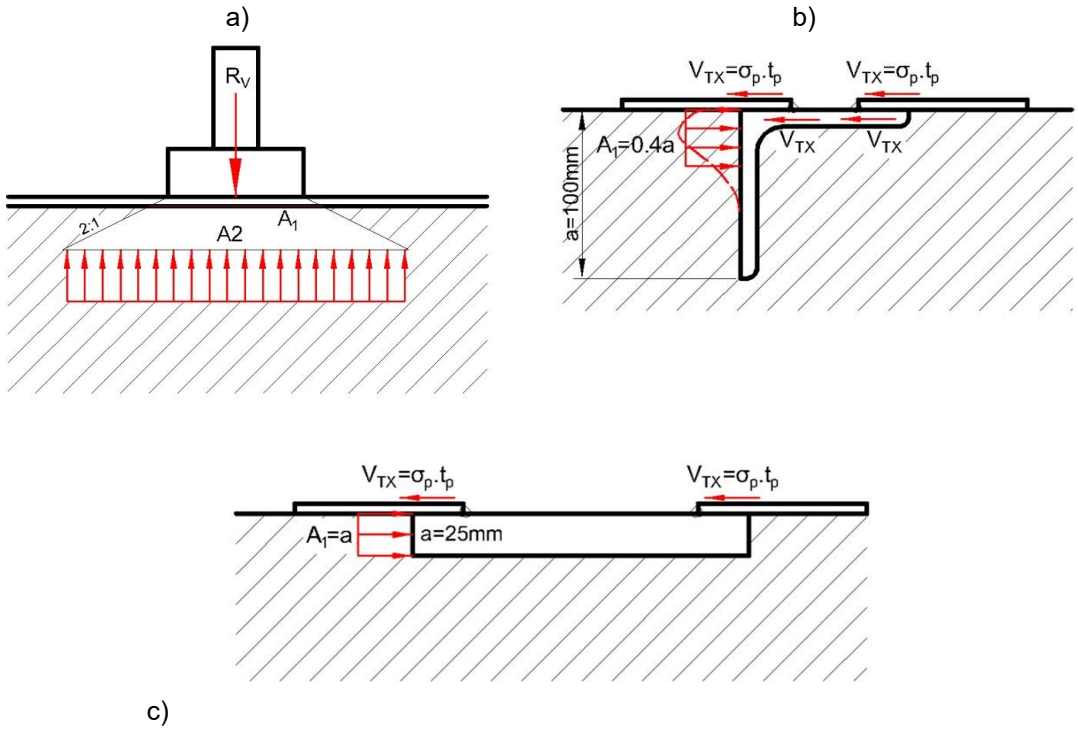

Figure 9. Liner components failure modes – a) Concrete crushing due to rack rocking (FM2, FM5); b) Embedded angle weld failure (FM9) and concrete crushing (FM10); c) Anchor plates bearing failure (FM7) and weld failure (FM8)

Estimated fragilities

Due to the limitation of the paper volume, detailed calculations for the liner components fragilities are not presented. The parameters of the liner components fragilities are summarised in Table 2.

FM	Failure type	A_m, g	β_R	β_U	β_C	A_{HCLPF}, g
FM1a	Liner plate tearing @ floor-wall joint	6.11	0.31	0.35	0.47	2.06
FM1b	Liner plate tearing @ anchor plate	4.62	0.31	0.35	0.47	1.56
FM2	Concrete bearing under liner	4.60	0.31	0.41	0.51	1.41
FM5	*Concrete bearing under base plate*	*2.88*	*0.31*	*0.41*	*0.51*	*0.88*
FM7	Concrete bearing of anchor plate	4.46	0.31	0.41	0.51	1.36
FM8	Liner plate to anchor plate weld	3.69	0.31	0.36	0.48	1.23
FM9	Liner plate to embedded angle weld	5.67	0.31	0.36	0.48	1.88
FM10	Concrete bearing of embedded angles	6.51	0.31	0.41	0.51	1.99

Table 2. Parameters of the liner components fragilities

The liner component failure mode with minimum median capacity and HCLPF capacity is FM5 "C ncrete bearin under ba e ate" wit A_m=2.88g and A_{HCLPF}=0.88g. The failure mode with the second minimum HCLPF capacity is FM8 with A_m=3.69g and A_{HCLPF}=1.23g. All mean component fragility functions are plotted in Figure 10.

Correlation of failure modes

In the calculation of seismic fragilities presented above, no correlation was assumed between different failure modes for a single liner component, or between failure modes for different components. Based on the definition of the failure modes, this assumption is valid *per se* for failure modes that are triggered in different critical locations and by different load/stress components. Possibility for failure correlation exists for failure modes that are triggered by the same load/stress components and have the same critical locations for failure initiation. For the case of the SFP liner, based on the performed fragility analysis, possible correlation exists for stress transfer from liner plate to embedded angles: correlation between failure modes 1a, 9, and 10. A simplified approach for common cause adjustment using the already calculated fragility functions was used to assess the effect of failure mode correlation. The approach uses the theorem of uni-modal limits as presented by Ang & Tan (1984).

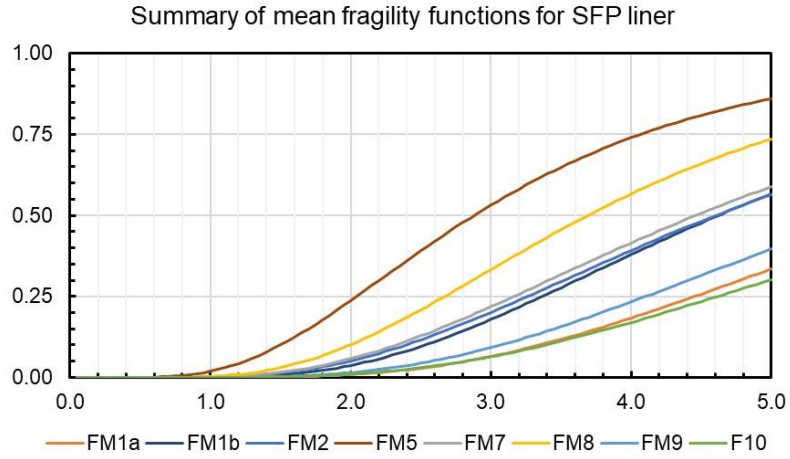

Figure 10. Summary of mean fragility functions for failure of liner components

Since the fragility functions for the non-correlated failure modes FM1a, 9 and 10 are log-normally di tributed wit very c e uncertainty va ue (β_c= -0.51) and similar median capacities (5.676.51g), the calculated correlated fragility function is well fitted to log-normal distribution with A_m= and β_c=0.37. The estimated HCLPF for the correlated failure modes is 1.71g, which is about 8% less than the minimum HCLPF of the three failure modes without correlation and significantly higher than the minimum HCLPF for FM5.

Conclusions

The SFP reinforced concrete structure was demonstrated to be robust against earthquakes with calculated conservative deterministic HCLPF value 2.05g or 3.4 times higher than the Reference Earthquake. The critical failure mode of the structure is shear of the SFP floor. Such shear will

lead to gross structural failure and uncontrollable loss of SFP inventory water. The SFP stainless steel liner is less robust against earthquakes but still has capacity above the Reference Earthquake level. The two failure modes with highest probabilistically estimated seismic fragilities are: M “C ncrete bearin ai ure be w t e exi tin ba e ate ” (CL = and M “Liner ate t anc r ate we d ai ure” (CL = 3 B t ai ure wi l potentially affect localised areas of the SFP floor liner. Failure modes of liner components with potential to lead to rapid and uncontrollable loss of inventory water have significantly higher HCLPF capacities.

References

EPRI TR-3002009564, *Seismic Evaluation Guidance: Spent Fuel Pool Integrity Evaluation*, Electric Power Research Institute, 2017

EPRI TR-3002012994, *Seismic Fragility and Seismic Margin Guidance for Seismic Probabilistic Risk Assessments*, Electric Power Research Institute, 2018

ASCE 4-16, *Seismic Analysis of Safety-Related Nuclear Structures and Commentary*, American Society of Civil Engineers, 2017

ACI 349M-13, *Code Requirements for Nuclear Safety-Related Concrete Structures and Commentary. SI Edition*, American Concrete Institute, 2013

ACI 350.3-06, *Seismic Design of Liquid Containing Concrete Structures and Commentary*, American Concrete Institute, 2013

AISC N690, *Specification for Safety-Related Steel Structures for Nuclear Facilities, incl. Supplement No. 1*, American Institute for Steel Construction, 2013

ANSI/ANS-57.7, *Design Criteria for an Independent Spent Fuel Storage Installation (Water Pool Type)*, American National Standards Institute, 1988 (R1997), withdrawn standard

Ang A H-S and Tang WH (1984), *Probability concepts in engineering planning and design. Volume 2: Decision, Risk And Reliability*, New York: John Wiley & Sons

Genov Ts, Travanca JP, Andreev S and Andonov A (2023), Nonlinear seismic analysis of a spent fuel pool considering structure-fluid-structure interaction, *SECED23 Conference*, Cambridge, UK